Virtual calibration of whole-body counter using a library of statistical phantoms

Laleh Rafat-Motavalli, Elie Hoseinian-Azghadi, and Hashem Miri-Hakimabad*
Physics Department, Faculty of Science, Ferdowsi University of Mashhad, Mashhad, Iran
*Corresponding author: mirihakim@um.ac.ir

***Abstract*—In this study, virtual calibration of a whole-body monitoring system was performed using a library of 100 statistical phantoms. The counting efficiency (CE) was obtained as a function of time after ^{131}I radionuclide intake. The results highlight the necessity of using statistical phantoms in the process of virtual calibration because it was found that the CE for ^{131}I is not a simple function of height, weight, BMI or any other morphometric variable. Despite, it was shown that the counting efficiency is strongly dependent on the geometrical location of the thyroid and the thickness of soft tissue between the thyroid and the detectors.**

***Index Terms*—whole-body counter; Monte Carlo method; virtual calibration; statistical phantoms, radiation contamination**

I. Introduction

In the virtual calibration of in vivo monitoring instruments, computational phantoms which include the complicated structure of human anatomy are used to assess the organ specific counting efficiency (OSCE) [1]. Although utilizing a realistic computational phantom instead of simple physical models increases the accuracy; without personalized models, this method has another source of uncertainty pertained to the anatomical variations in measurement subjects [2]. Therefore, some researchers created phantom libraries comprising of various weight and height percentiles to take into account the statistical uncertainty of the morphometric features. However, because of lacking the anatomical information, the internal organs were assumed identical for the same height phantoms. To make the other height percentiles, all the organs were just scaled with the whole body [3]. This issue could effectively contribute to the systematic error in OSCE estimation, especially when contamination is concentrated in a specific organ. In this work, a library of 100 phantoms with internal and external statistical features were used to calibrate a whole body counter (WBC) for ^{131}I which is assumed to be predominant contributor to the internal dose after a nuclear power plant accident.

II. Methods

A. Simulating of statistical phantoms inside the WBC

The phantom series used in this study were constructed as a library of 100 statistical boundary representation phantoms. The sampling of height and weight of the patients were done uniformly and including adult males and females.

A FASTSCAN WBC unit (Canberra Inc., USA) was simulated in MCNPX 2.6 code which has a free standup geometry. The unit houses two sodium iodide (NaI) gamma-ray detectors [4].

B. Biokinetics of radiation contamination in body

The compartmental biokinetic model of the inhaled 131I was created as a combination of human respiratory tract model (HRTM) from ICRP Publication 130 [5] and the new iodine biokinetic model developed by Leggett [6]. The activity curves versus time after intake were then obtained for inhalation of iodine vapor/gases I_2, CH_3I, and aerosols with AMAD of 1 and 5μm. In addition, the solutions of biokinetic model for blocked and unblocked thyroid as well as various breathing rates and durations were found.

C. Evaluation of CE

The OSCE, ε_S, were evaluated and the total CE, ε_{Total}, were then obtained as a summation of $\sum A_S(t) \times \varepsilon_S$ for each computational phantom, where $A_S(t)$ is the activity function for the source region (S).

III. Results and Discussion

A. The total CE and OSCEs for the reference phantom

Monte Carlo simulation was performed and organ specific CEs were obtained for 15 different source regions, separately. The total CE were then obtained by summing the activity-weighted organ-specific CEs. Figure 1 shows the total CE for the adult male ICRP reference phantom as a function of time after inhalation of ^{131}I aerosols with 1 μm AMAD. The

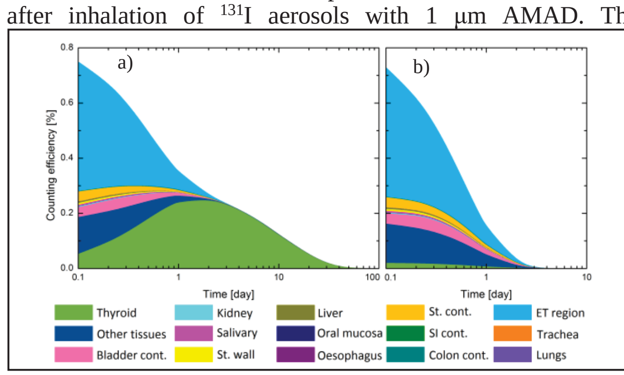

Figure 1. Total CE as a function of time after intake of ^{131}I aerosols with 1 μm AMAD for a reference subject with (a) unblocked and (b) blocked thyroid.

contribution of each source region in the total CE is shown for both blocked and unblocked thyroid in this figure. In the case of unblocked thyroid, the key point is that the thyroid is the major contributor to the total CE after 2 days of radionuclide intake. This implies that the thyroid could be considered alone in the evaluation of total CE. However for blocked thyroid, it was shown that the CE is not considerable after 2 days.

B. The total CE for the library of statistical phantoms

The total CEs for 100 statistical phantoms were evaluated (figure 2). Figure 3 shows the scatter plot of weight versus height of the computational phantoms. The symbols filled with the color corresponding to the thyroid CE as the major contributor to the total CE. The polygon mesh models of the phantoms pertained to the region indicated with a dashed magenta line was shown in the upper panel from the front view. As can be seen from this figure, there is no obvious correlation between the thyroid CE and its corresponding weight/height percentile.

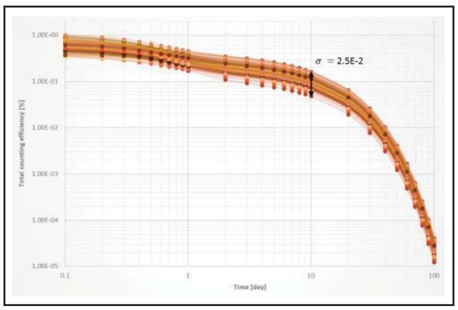

Figure 2. Total CE as a function of time after intake of ^{131}I aerosols with 1 μm AMAD for the library of computational phantoms.

C. The total CE vs. other morphmetric parameters

The correlation between thyroid CE versus various parameters including body mass index (BMI) and thyroid mass were investigated and no obvious correlation was found. Then, we explored more deeply and some level of correlation was observed for the thyroid location with respect to the detectors. Therefore, we analytically estimated the solid angle (Ω) of the detectors observed from the thyroid center of mass, multiplied by the attenuation factor (exp(-μx)), where x is the thickness of the soft tissue lied in front of the thyroid and μ is the attenuation coefficient of the soft tissue for energy of 0.365 MeV. One may expect that the value would be proportional to the thyroid CE as shown in figure 4.

To sum up, the total CE is dependent on the thyroid CE after 2 days of radionuclide intake, which in turns depends on the thyroid location and the thickness of thyroid frontal layer. Thus, in order to estimate the total CE for each individual subject more precisely, one may fix the location of the thyroid by a neck or chin stabilizer and assess the thickness of soft tissue layer by palpation.

I. CONCLUSION

The total CE for ^{131}I as a function of time after intake were evaluated for different scenarios using a library of phantoms, new biokinetics of iodine and Monte Carlo calculations. The influencing factors on the total CE were also investigated.

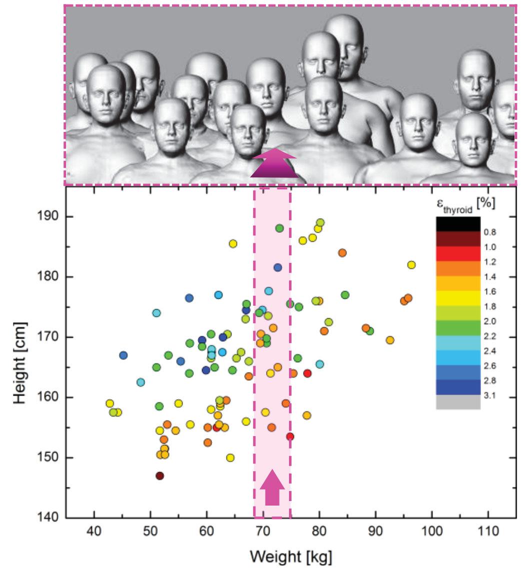

Figure 3. Scatter plot of height versus weight of the phantoms. the symbols filled with the color corresponding to the thyroid CE.

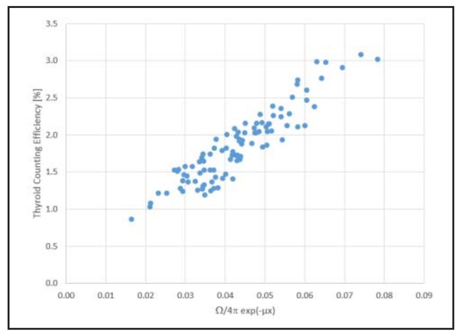

Figure 4. The correlation observed between the thyroid CE and the detercors' solid angle multiplied by attenuation factor for ^{131}I aerosols with 1 μm AMAD, plotted

The outcome of this study helps us to reduce the systematic uncertainty of CE pertained to the body habitus of the subject. To conclude, this study highlights the importance of using statistical phantoms in virtual calibration of whole body monitoring systems which we intend to share with computational phantoms workshop.

REFERENCES

[1] J. G. Hunt, and L. Bertelli, "Calibration of in vivo measurement systems and evaluation of lung measurement uncertainties using a voxel phantom," *Radiat Prot Dosim* vol. 76, pp. 179–84, 1998.

[2] S. Pölz, and B. Breustedt, "Personalised body counter calibration using anthropometric parameters," *Radiat Prot Dosim*, vol. 70(1-4), pp. 221-224, 2016.

[3] Y. Chen, R. Qiu, C. Li, Z. Wu, and J. Li, "Construction of Chinese adult male phantom library and its application in the virtual calibration of in vivo measurement," *Phys Med Biol*, vol. 61(5), pp. 2124, 2016.

[4] R. Hayano. "Measurement and communication: what worked and what did not in Fukushima", *Ann ICRP*, vol. 45(2_suppl), pp. 14-22, 2016.

[5] F. Paquet, G. Etherington, M. R. Bailey, R. W. Leggett, J. Lipsztein, et al., "ICRP Publication 130: Occupational Intakes of Radionuclides: Part 1," *Ann ICRP*, vol. 44(2), pp. 5-188, 2015.

[6] R. Leggett, "An age-specific biokinetic model for iodine," *J Radiol Prot*, vol. 37(4), pp. 864-882, 2017.